AIP | Applied Physics Letters

Effects of controllable biaxial strain on the Raman spectra of monolayer graphene prepared by chemical vapor deposition

Wenjing Jie, Yeung Yu Hui, Yang Zhang, Shu Ping Lau, and Jianhua Hao

Citation: Appl. Phys. Lett. **102**, 223112 (2013); doi: 10.1063/1.4809922
View online: http://dx.doi.org/10.1063/1.4809922
View Table of Contents: http://apl.aip.org/resource/1/APPLAB/v102/i22
Published by the AIP Publishing LLC.

Effects of controllable biaxial strain on the Raman spectra of monolayer graphene prepared by chemical vapor deposition

Wenjing Jie, Yeung Yu Hui, Yang Zhang, Shu Ping Lau, and Jianhua Hao[a)]
Department of Applied Physics, The Hong Kong Polytechnic University, Hung Hom, Hong Kong, People's Republic of China

(Received 9 April 2013; accepted 25 May 2013; published online 6 June 2013)

Controllable biaxial strain is delivered to monolayer graphene prepared by chemical vapor deposition via applying an electric field to the underlying piezoelectric $[Pb(Mg_{1/3}Nb_{2/3})O_3]_{0.7}$-$[PbTiO_3]_{0.3}$ substrate. The effects of tunable strain on the Raman spectra of graphene are investigated in reversible and real-time manners. Such strain can result in a blue shift in 2D band of graphene. The calculations based on the Grüneisen parameter identify the actual biaxial strain to graphene, leading to a continuous 2D band shift, which is detected during the retention of bias voltage. The physical mechanism behind this unique Raman behavior is discussed. © *2013 AIP Publishing LLC*. [http://dx.doi.org/10.1063/1.4809922]

Graphene has attracted tremendous attention because of its fascinating optical, electrical, and mechanical properties. A variety of graphene-related materials have been explored for a wide-range of applications.[1,2] Strain engineering in graphene is extensively studied because of the possibility of introducing a gap to graphene.[3,4] It has been proven to be feasible to impose uniaxial strain to graphene by stretching or bending the graphene-coated flexible substrates including polydimethylsiloxane (PDMS),[5] polymethyl methacrylate (PMMA)[6] and polyethylene terephthalate (PET).[7,8] However, these investigations are limited to uniaxial strain, and such type of strain is relatively large. Furthermore, it is difficult to study the Grüneisen parameters of graphene under uniaxial strain by considering such strain can move the relative position of Dirac cones.[9] Comparatively, biaxial strain is more suitable to study the strain effects on the vibrational properties.[10–12] Nevertheless, previous investigations of biaxial strain focused mainly on the mechanically exfoliated graphene (i.e., single-crystal graphene). Generally, chemical vapor deposition (CVD) synthesized large-area graphene sheets are polycrystalline and usually continuous, which are of great interest for industrial scale applications. However, the vibrational properties of CVD-grown graphene under biaxial strain are still lacking until now.

On the other hand, single-crystal $(1\text{-}x)[Pb(Mg_{1/3}Nb_{2/3})O_3]$-$x[PbTiO_3]$ (PMN-PT) is an excellent substrate which is capable of providing relatively large strain due to its giant electromechanical or converse piezoelectric response.[13,14] In our recent study, both light and ultrasound emissions have been observed in a single system of ZnS: Mn/PMN-PT.[15] The substrate-induced biaxial strain can be delivered to the as-prepared films and can dramatically affect the properties of the above layers. In this work, we have studied the vibrational behaviors of CVD-grown monolayer graphene under biaxial strain by directly transferring the graphene onto PMN-PT substrates. Such strategy provides a unique approach to investigate *in-situ* dynamically the Raman spectra of the graphene via piezoelectric-induced biaxial strain.

Monolayer graphene samples were prepared by CVD methods on copper foils and then transferred onto PMN-PT substrates. The detailed growth and transfer methods can be referred to our earlier work.[16] Before transfer process, oxygen plasma treatment was employed to enhance the hydrophilicity of the PMN-PT surface, which could make the graphene and the underlying PMN-PT form good adhesion. 150 nm-thick Au top electrodes were deposited directly on the graphene sheet by thermal evaporation, while the backside of the PMN-PT substrate was coated with Au to form bottom electrode. The resistance of graphene is about several kΩ, which is much smaller than that of the underlying PMN-PT. Hence, the large-area continuous graphene layer served as a top electrode to form the parallel plate capacitor when a bias voltage was applied to the PMN-PT. The schematic of the hybrid system is shown in Fig. 1(a). High resolution X-ray diffractometer (XRD) (Rigaku, SmartLab, 9 kW) equipped with a Ge (220) 2 bounce monochromator was used to get 2θ scanning patterns of the PMN-PT. The graphene layer was characterized using Raman spectroscopy (HORIBA, HR800) with the excitation wavelength of 488 nm and the laser spot size of 1 μm. A Keithley 2410 SourceMeter was introduced to provide bias voltage. Prior to the measurements, we positively polarized the PMN-PT substrate by applying an electric field (E) of 10 kV/cm to the substrate, resulting in the electric dipole moments pointing towards the graphene sheet. Additionally, the polarization hysteresis loop was measured under an ac electric field with 10 Hz using a conventional Sawyer–Tower circuit. All the above measurements were performed in air ambient at room temperature.

The Raman spectrum of graphene on the PMN-PT substrate is shown in Fig. 1(b). The most intense features of G and 2D peaks, corresponding to the doubly degenerate E_{2g} phonon at the Brillouin zone center and the second order of the D peak, respectively, can be clearly observed. A symmetric 2D peak lies at about 2700 cm^{-1}, with full-width-at-half maximum (FWHM) of about 40 cm^{-1}. The intensity of the 2D peak is found to be approximately 2 times of that of the G peak, indicating that the graphene is single-layer. No defect-related D peak (due to the breathing modes of

a)Author to whom correspondence should be addressed. Electronic mail: jh.hao@polyu.edu.hk

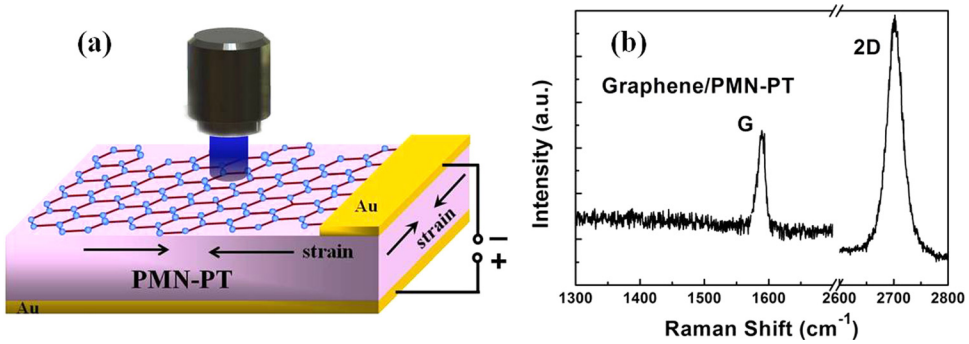

FIG. 1. (a) Schematic of graphene/PMN-PT hybrid system. (b) Raman spectrum of graphene on PMN-PT substrate.

six-atom rings and requires a defect for its activation) is observed, confirming the absence of significant defects in the graphene sheet. The mapping images of Raman spectra in terms of both position and intensity from graphene feature peaks are shown in Fig. 2. After the applied strain is removed, almost same mapping image can be obtained. The defect-related D band is still invisible after removing the strain, which also rules out the possibility of generating defects such as slipping and buckling in graphene by the strain.

XRD technique was used to analyze the lattice deformation of PMN-PT. As shown in Fig. 3(a), the (002) diffraction peak of PMN-PT shows a visible shift when the hybrid structure is applied by dc voltages, and more importantly, with increasing the applied voltage, the (002) peak shifts towards lower angles. The inset of Fig. 3(a) shows the position of (002) peak of PMN-PT as a function of the applied voltage. Evidently, the PMN-PT substrate can produce out-of-plane tensile strain. In other words, the in-plane strain is compressive. According to the Bragg's law and Poisson ratio, the in-plane strain can be calculated.[17] The substrate-induced strain has a linear dependence on the bias voltage with a slope of −0.04% per 100 V. Fig. 3(b) shows the 2D peaks of the graphene shift to higher frequency as the applied voltage increases from 100 to 600 V. This shift in Raman peak is usually caused by the distortion of the graphene lattice, which can alter the vibrational properties of the phonons within the lattice. The 2D band shift ($\Delta\omega_{2D}$) is exhibited as a function of the applied strain in the inset of Fig. 3(b). Typically, compressive biaxial strain leads to a phonon hardening (blue shift) for single-crystal graphene, while tension leads to phonon softening (red shift).[10,11] In our experiments, the 2D peaks also show blue-shifted characteristics under compressive strain. Negative voltages also give rise to the left shifts of (002) peaks in the XRD patterns shown in Fig. 4(a), indicating a compressive strain is produced by a negative bias voltage, which is consisted with previous reports for PMN-PT.[18,19] Such compressive strain also induces the blue shifts of 2D Raman band from 2703 to 2714 cm^{-1} as shown in Fig. 4(b).

However, the position of Raman feature peaks is also carrier dependent.[20,21] Earlier studies reported that carrier doping can usually lead to the decrease in intensity of 2D band and line broadening in 2D peak, accompanied by the low ratio (usually less than 1) of $\Delta\omega_{2D}/\Delta\omega_G$ ($\Delta\omega_{2D}$ is the shift of 2D band frequency, while $\Delta\omega_G$ is the shift of G band).[22] As shown in Fig. 3(b), the 2D peaks of the graphene show a blue shift as the applied voltage increases, while both the intensity and the FWHM of 2D peak show weak dependence on the applied voltage. In addition, the 2D peak shift is over 2 times more than G peak shift under the same bias voltage as shown in Fig. 4(d). The inset of Fig. 4(d) exhibits the shift of G peak ($\Delta\omega_G$) as a function of the voltage. The G peak shifts about 2.4 and 4.3 cm^{-1}, corresponding to about 5.6 and 9.6 cm^{-1} for 2D peak, under bias voltage of 400 and 600 V, respectively. Furthermore, the position of the 2D peak calculated through density functional theory (DFT) framework does not change much even at high hole doping level (hole density of 10^{13} cm^{-2}).[21] In fact, the carrier concentration is relatively low considering the thickness of PMN-PT is 0.5 mm. Besides that, the 2D band position shows a V-shape curve as a function of the bias voltage in our experiments as shown in Fig. 4(c), which is in conflict with the 2D band shift behaviors induced by carrier doping. All the above analysis suggests that the effect of carrier doping on the 2D band shift is negligible compared to the compressive strain effect.

It should be pointed out that the strain exerted on the graphene is not exactly the strain provided by the underlying

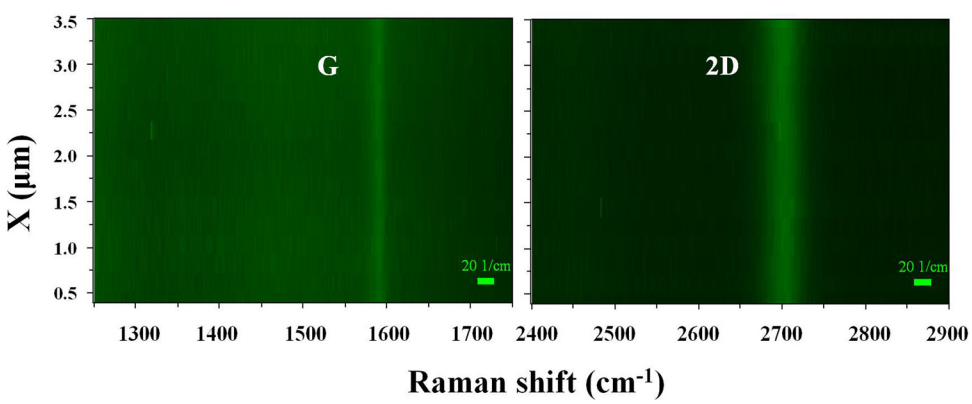

FIG. 2. Raman spectra mapping images of feature peaks of graphene over an area of 3 $\mu m \times 6$ μm.

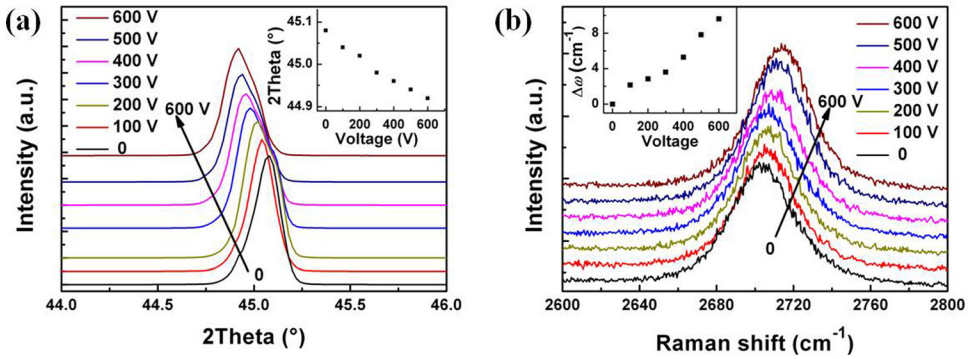

FIG. 3. (a) The PMN-PT (002) peaks of XRD 2θ scanning patterns with bias voltage changed from 0 to 600 V. The position of (002) peak at different voltage is shown in the inset. (b) 2D peaks of graphene under different bias voltage varied from 0 to 600 V. Inset shows the shift of 2D band as a function of voltage.

substrate owing to the inefficient interfacial compressive strain transfer.[23] Based on the Raman 2D peak shift, we can use the Grüneisen parameter for 2D band to identify the actual strain applied to the graphene. The specific 2D band position can be obtained by fitting the 2D peak with single-peak Lorentzian functions. The 2D peak shifts towards higher frequency by about 1.5 cm^{-1} because of the in-plane strain induced by a bias voltage of 100 V. The Grüneisen parameter is defined as

$$\gamma = -1/(2\omega_0)\ \partial\omega/\partial\varepsilon, \tag{1}$$

where ω_0 and ω are Raman frequencies at zero strain and finite biaxial strain, respectively. ε is the biaxial strain. Here, for the 2D band, the $\Delta\omega_{2D}$ can be expressed as

$$\Delta\omega_{2D} = -2\omega_0\gamma_{2D}\varepsilon. \tag{2}$$

The Grüneisen parameter for 2D band derived from mechanically exfoliated graphene can be applied to the CVD-grown polycrystalline graphene,[23] when considering that the 2D band is affected only by the strain from inside of the grains.[24–26] In this work, we use the Grüneisen parameter for 2D band derived from the shift of Raman peak by Zabel *et al.* to be 2.6 ± 5%.[11] This value is in good agreement with the Grüneisen parameter (2.7) calculated from first principles by Mohiuddin *et al.*[9] Herein, we obtain the actual strain applied to the graphene to be about −0.011% per 100 V. Note that such strain magnitude is much smaller than that of the PMN-PT (−0.04%) based on the aforementioned XRD result, suggesting that the piezoelectric-induced in-plane strain might have not been completely transferred to the graphene sheet. This may be mainly attributed to the extremely high stiffness of graphene and the inefficient interfacial strain transfer.[23]

Next, we measured the 2D band of Raman frequency during the retention of a bias voltage (400 V) as shown in Fig. 5(a). The 2D peak shifts towards higher frequency by 6 cm^{-1} as the bias voltage is applied to the hybrid system. After the immediate blue shift, 2D peak shifts steadily to higher frequency with a further shift of about 4 cm^{-1}. Then, after about 60 min, the shift is saturated. As shown in Fig. 5(b), the evolution of the 2D peak shift can be divided into three regions as I, II, and III, which correspond to jumping, steadily increased and saturated states, respectively. Based on the 2D Raman peak shift, the strain introduced to the graphene can be calculated. The voltage of 400 V instantaneously imposes −0.043% strain to graphene, and subsequently, introduces a strain of −0.071% to the graphene. Furthermore, the

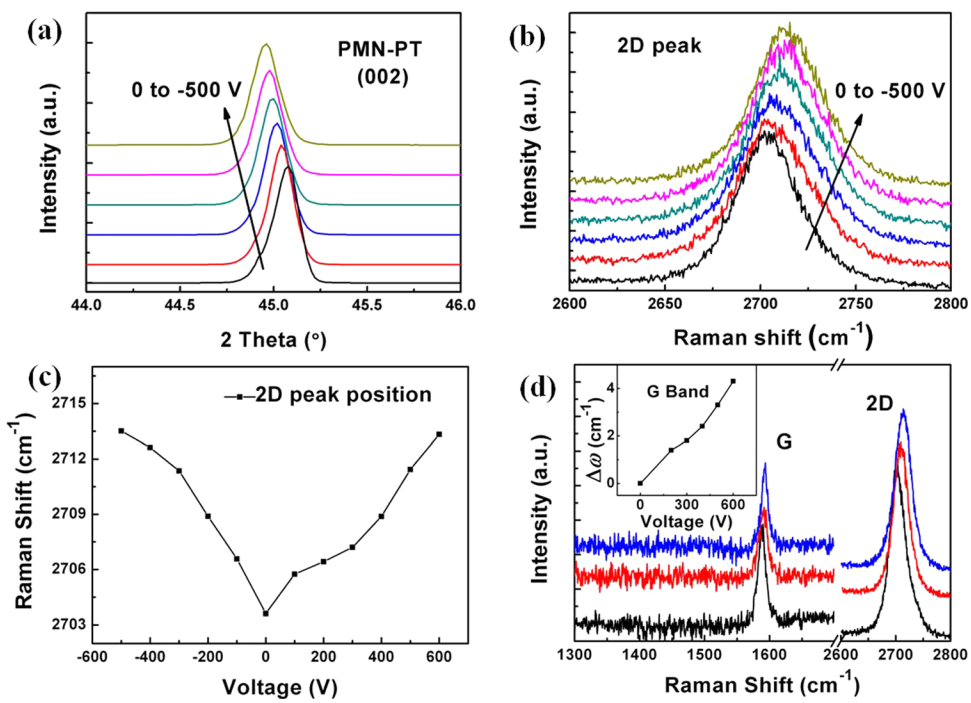

FIG. 4. (a) The PMN-PT (002) peaks of XRD 2θ scanning patterns with bias voltage changed from 0 to −500 V. (b) The 2D peaks of Raman spectra with bias voltage varied from 0 to −500 V. (c) The 2D band position as a function of the applied voltage from −500 to 600 V. (d) Raman feature peeks of G and 2D for graphene under different bias voltage. The shift of G band as a function of voltage is shown in the inset.

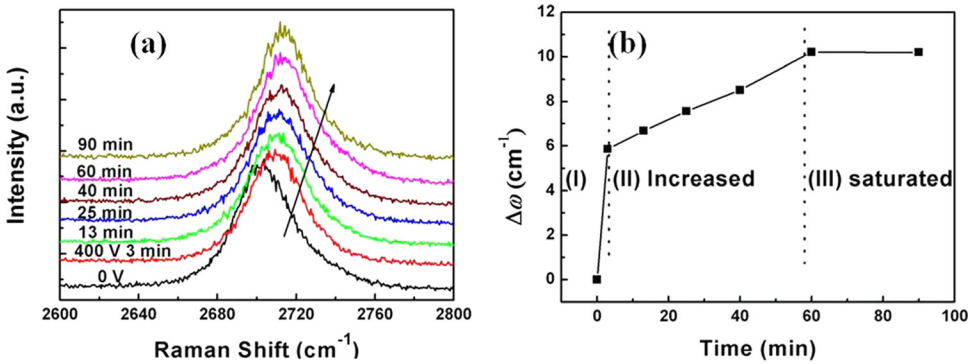

FIG. 5. (a) Raman spectra response to a bias voltage of 400 V at different time. (b) The 2D peak shift as a function of time during the retention of the applied external *E*.

PMN-PT under a bias voltage of 400 V was measured by the XRD technique and the position of (002) peak is time-independent when the bias voltage keeps constant (not shown in this paper), which implies that the strain provided by the underlying substrate remains constant. However, the strain exerted on the graphene is time-dependent. One possible reason for such unique behavior could be the different strain distribution between grains and grain boundaries in CVD-grown graphene. Note that the grain size of polycrystalline graphene grown on copper foils ranges from several hundred nm to several μm, which is comparable with the spot size (1 μm). So, when performing Raman spectroscopy of CVD-grown graphene, there is a high possibility of detecting grain boundaries.[23] It is reported that grain boundaries can reduce the stiffness of graphene. As a consequence, strain in grain boundaries is larger than that inside grains.[24,25] The larger strain in grain boundaries would be likely to introduce the additional increase of strain inside the grains, corresponding to the continuous blue shift in 2D band. Additionally, reproducible experimental results still exhibit the continuous Raman shift.

In summary, we present the *in-situ* and real-time Raman spectra of graphene under controllable biaxial strain based on graphene/PMN-PT hybrid system. The PMN-PT substrate could impose compressive biaxial strain to graphene under a bias voltage and result in a blue shift in the 2D band. The actual amount of biaxial strain exerted on the graphene layer is calculated. After the initial response to the applied voltage, a continuous blue shift can be detected during the retention of bias voltage.

[1]A. K. Geim and K. S. Novoselov, Nature Mater. **6**, 183 (2007).
[2]X. Huang, Z. Yin, S. Wu, X. Qi, Q. He, Q. Zhang, Q. Yan, F. Boey, and H. Zhang, Small **7**, 1876 (2011).
[3]S.-M. Choi, S.-H. Jhi, and Y.-W. Son, Phys. Rev. B **81**, 081407(R) (2010).
[4]G. Cocco, E. Cadelano, and L. Colombo, Phys. Rev. B **81**, 241412(R) (2010).
[5]X.-W. Fu, Z.-M. Liao, J.-X. Zhou, Y.-B. Zhou, H.-C. Wu, R. Zhang, G. Jing, J. Xu, X. Wu, W. Guo, and D. Yu, Appl. Phys. Lett. **99**, 213107 (2011).
[6]O. Frank, G. Tsoukleri, J. Parthenios, K. Papagelis, I. Riaz, R. Jalil, K. S. Novoselov, and C. Galiotis, ACS Nano **4**, 3131 (2010).
[7]Z. H. Ni, T. Yu, Y. H. Lu, Y. Y. Wang, Y. P. Feng, and Z. X. Shen, ACS Nano **2**, 2301 (2008).
[8]Y.-H. Lee and Y.-J. Kim, Appl. Phys. Lett. **101**, 083102 (2012).
[9]T. M. G. Mohiuddin, A. Lombardo, R. R. Nair, A. Bonetti, G. Savini, R. Jalil, N. Bonini, D. M. Basko, C. Galiotis, N. Marzari, K. S. Novoselov, A. K. Geim, and A. C. Ferrari, Phys. Rev. B **79**, 205433 (2009).
[10]F. Ding, H. Ji, Y. Chen, A. Herklotz, K. Dörr, Y. Mei, A. Rastelli, and O. G. Schmidt, Nano Lett. **10**, 3453 (2010).
[11]J. Zabel, R. R. Nair, A. Ott, T. Georgiou, A. K. Geim, K. S. Novoselov, and C. Casiraghi, Nano Lett. **12**, 617 (2012).
[12]J.-U. Lee, D. Yoon, and H. Cheong, Nano Lett. **12**, 4444 (2012).
[13]S.-E. Park and T. R. Shrout, J. Appl. Phys. **82**, 1804 (1997).
[14]Z. Kutnjak, J. Petzelt, and R. Blinc, Nature **441**, 956 (2006).
[15]Y. Zhang, G. Gao, H. L. H. J. Dai, Y. Wang, and J. Hao, Adv. Mater. **24**, 1729 (2012).
[16]Y. Y. Hui, G. Tai, Z. Sun, Z. Xu, N. Wang, F. Yan, and S. P. Lau, Nanoscale **4**, 3118 (2012).
[17]R. Zheng, Y. Wang, J. Wang, K. Wong, H. Chan, C. Choy, and H. Luo, Phys. Rev. B **74**, 094427 (2006).
[18]E. J. Guo, J. Gao, and H. B. Lu, Europhys. Lett. **95**, 47006 (2011).
[19]Y. Yang, Z. L. Luo, H. Huang, Y. Gao, J. Bao, X. G. Li, S. Zhang, Y. G. Zhao, X. Chen, G. Pan, and C. Gao, Appl. Phys. Lett. **98**, 153509 (2011).
[20]S. Pisana, M. Lazzeri, C. Casiraghi, K. S. Novoselov, A. K. Geim, A. C. Ferrari, and F. Mauri, Nature Mater. **6**, 198 (2007).
[21]A. Das, S. Pisana, B. Chakraborty, S. Piscanec, S. K. Saha, U. V. Waghmare, K. S. Novoselov, H. R. Krishnamurthy, A. K. Geim, A. C. Ferrari, and A. K. Sood, Nat. Nanotechnol. **3**, 210 (2008).
[22]J. E. Lee, G. Ahn, J. Shim, Y. S. Lee, and S. Ryu, Nat. Commun. **3**, 1024 (2012).
[23]M. A. Bissett, W. Izumida, R. Saito, and H. Ago, ACS Nano **6**, 10229 (2012).
[24]J. Kotakoski and J. C. Meyer, Phys. Rev. B **85**, 195447 (2012).
[25]F. Hao and D. Fang, Phys. Lett. A **376**, 1942 (2012).
[26]L. M. Malard, M. A. Pimenta, G. Dresselhaus, and M. S. Dresselhaus, Phy. Rep. **473**, 51 (2009).